Electronic Supplementary Information for

First thermal studies on visible-light-switchable negative T-type photochromes of nitrile-rich series

Mikhail Yu. Belikov* and Mikhail Yu. Ievlev

Ulyanov Chuvash State University, Moskovskiy pr. 15, Cheboksary, Russia.

*E-mail: belikovmil@mail.ru

Contents

1. Kinetics of the dark reaction for compounds 1a and 1b at different temperatures (C = 2.5 × 10^{-5} M)

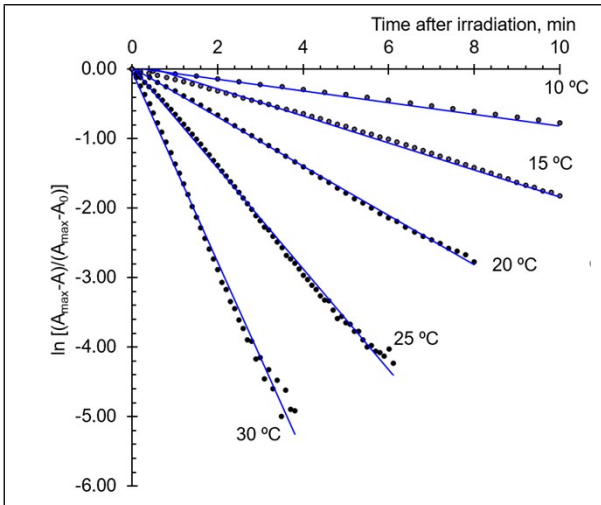

Fig. 1. Kinetics of the dark reaction for compound **1a** in EtOH at different temperatures

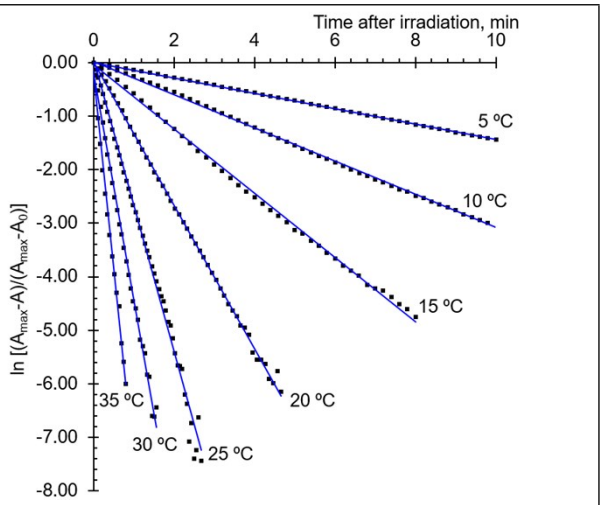

Fig. 2. Kinetics of the dark reaction for compound **1b** in EtOH at different temperatures

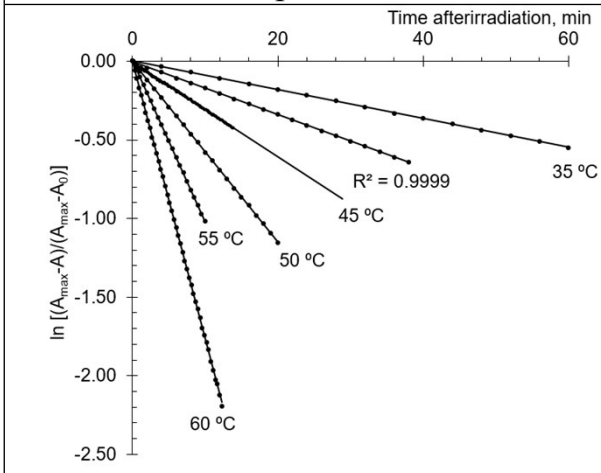

Fig. 3. Kinetics of the dark reaction for compound **1a** in DiOX at different temperatures

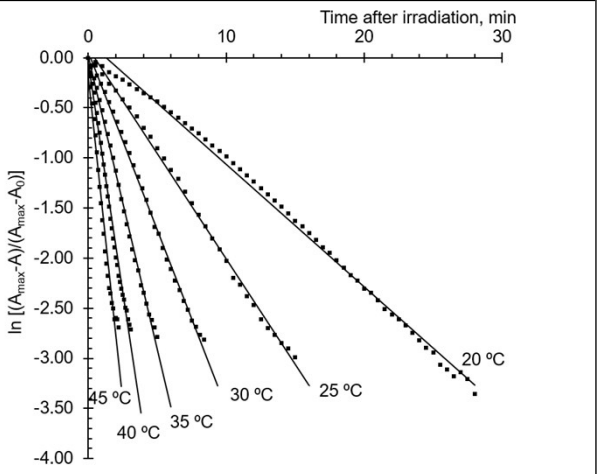

Fig. 4. Kinetics of the dark reaction for compound **1b** in DiOX at different temperatures

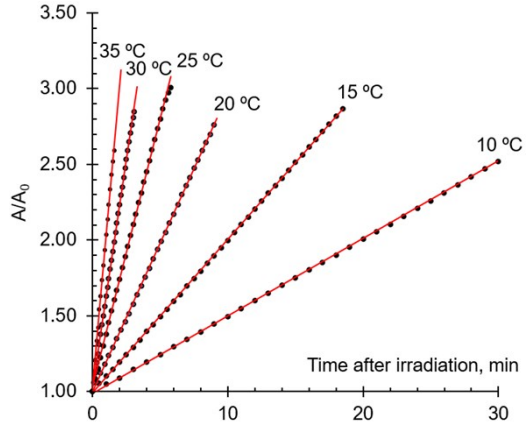

Fig. 5. Kinetics of the dark reaction for compound **1a** in MeCN at different temperatures

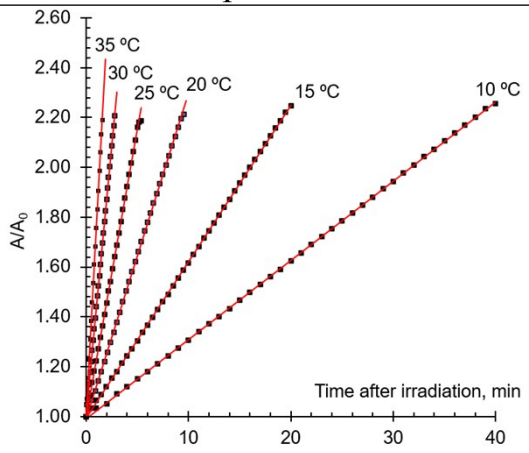

Fig. 6. Kinetics of the dark reaction for compound **1b** in MeCN at different temperatures

2. Relationship between the dark reaction rate constant and temperature for compounds 1a and 1b ($C = 2.5 \times 10^{-5}$ M)

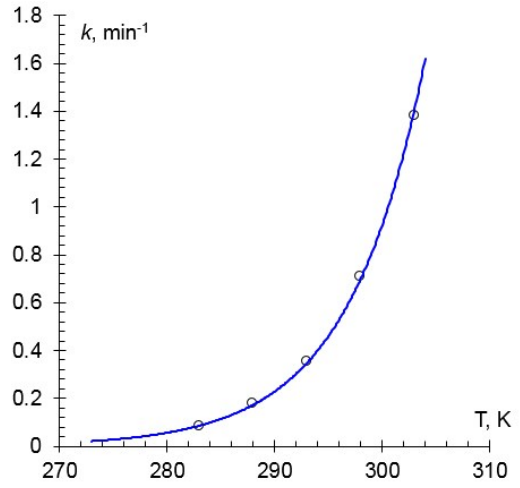

Fig. 7. Relationship between the dark reaction rate constant and temperature for compounds **1a** in EtOH

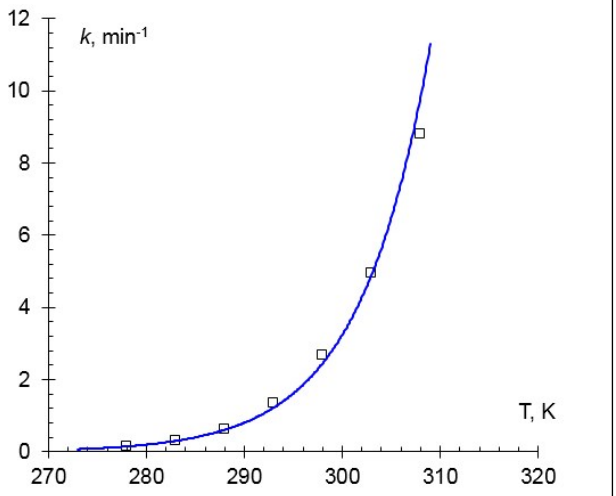

Fig. 8. Relationship between the dark reaction rate constant and temperature for compounds **1b** in EtOH

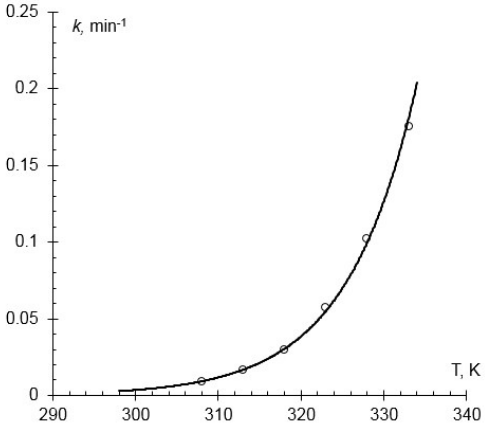

Fig. 9. Relationship between the dark reaction rate constant and temperature for compounds **1a** in DiOX

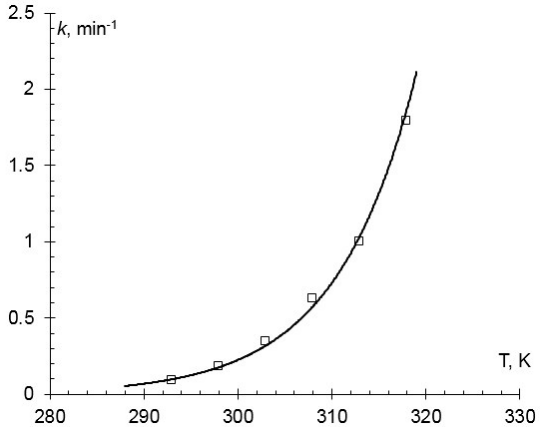

Fig. 10. Relationship between the dark reaction rate constant and temperature for compounds **1b** in DiOX

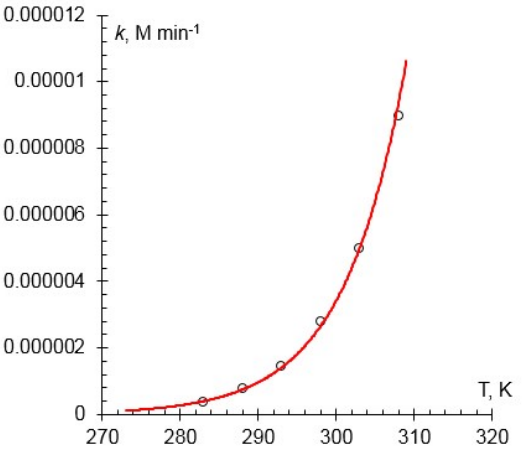

Fig. 11. Relationship between the dark reaction rate constant and temperature for compounds **1a** in MeCN

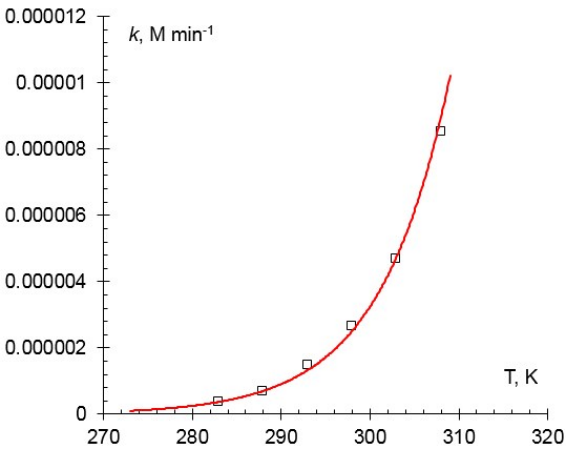

Fig. 12. Relationship between the dark reaction rate constant and temperature for compounds **1b** in MeCN

3. NMR ^{1}H, ^{13}C spectra

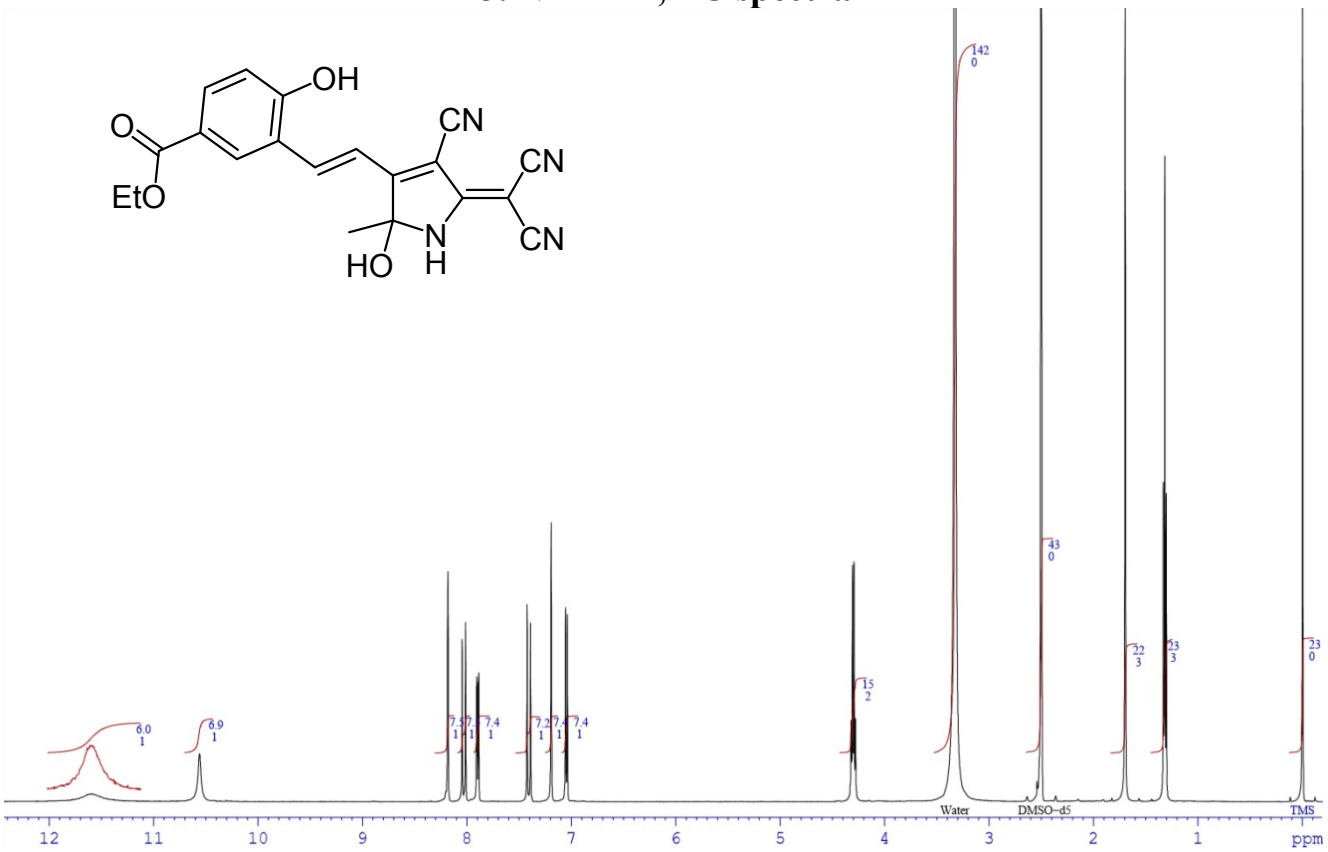

Fig. 13. ^{1}H-NMR-spectrum of compound **1a** (500 MHz, DMSO−d_6, 298K)

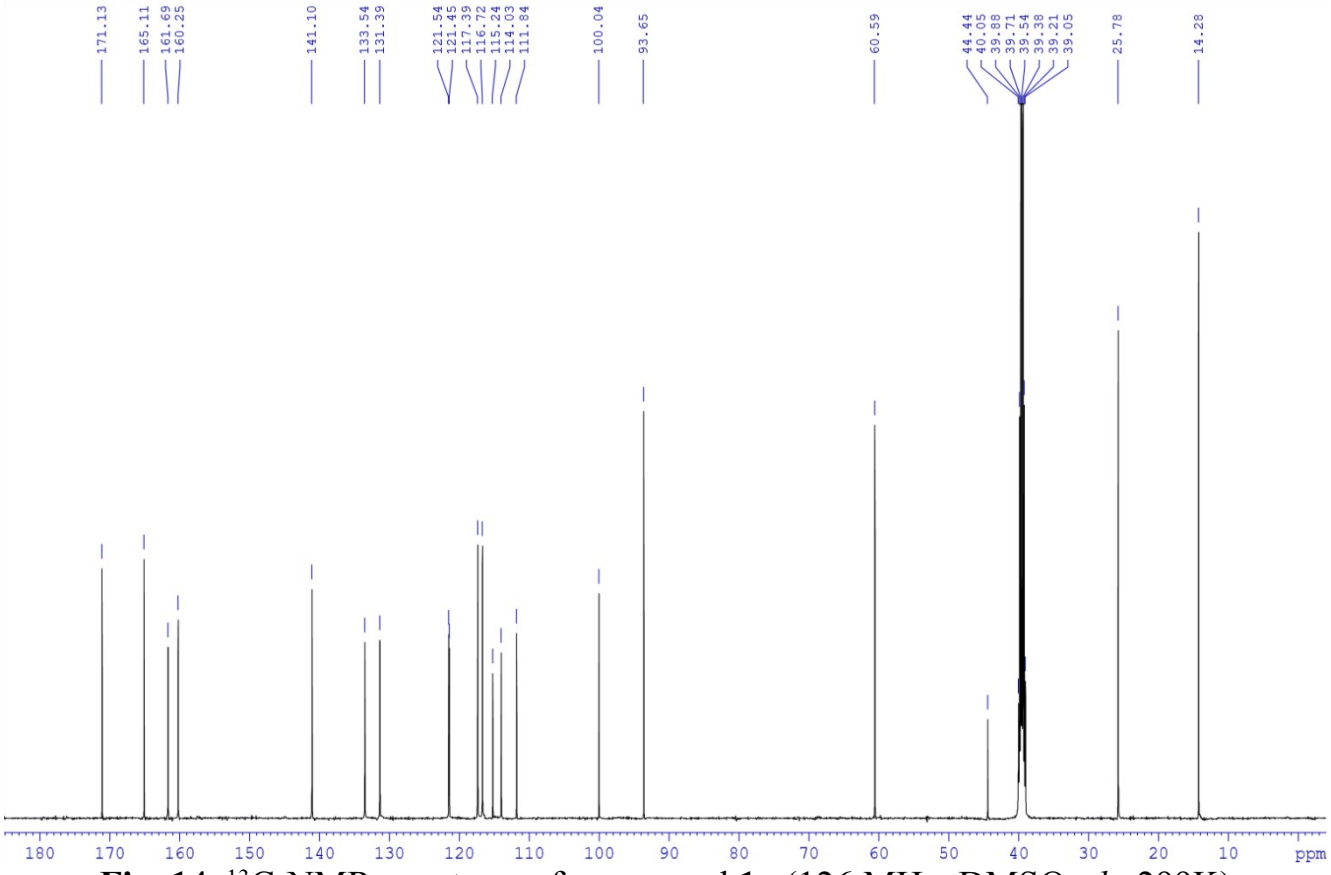

Fig. 14. ^{13}C-NMR-spectrum of compound **1a** (126 MHz, DMSO−d_6, 299K)

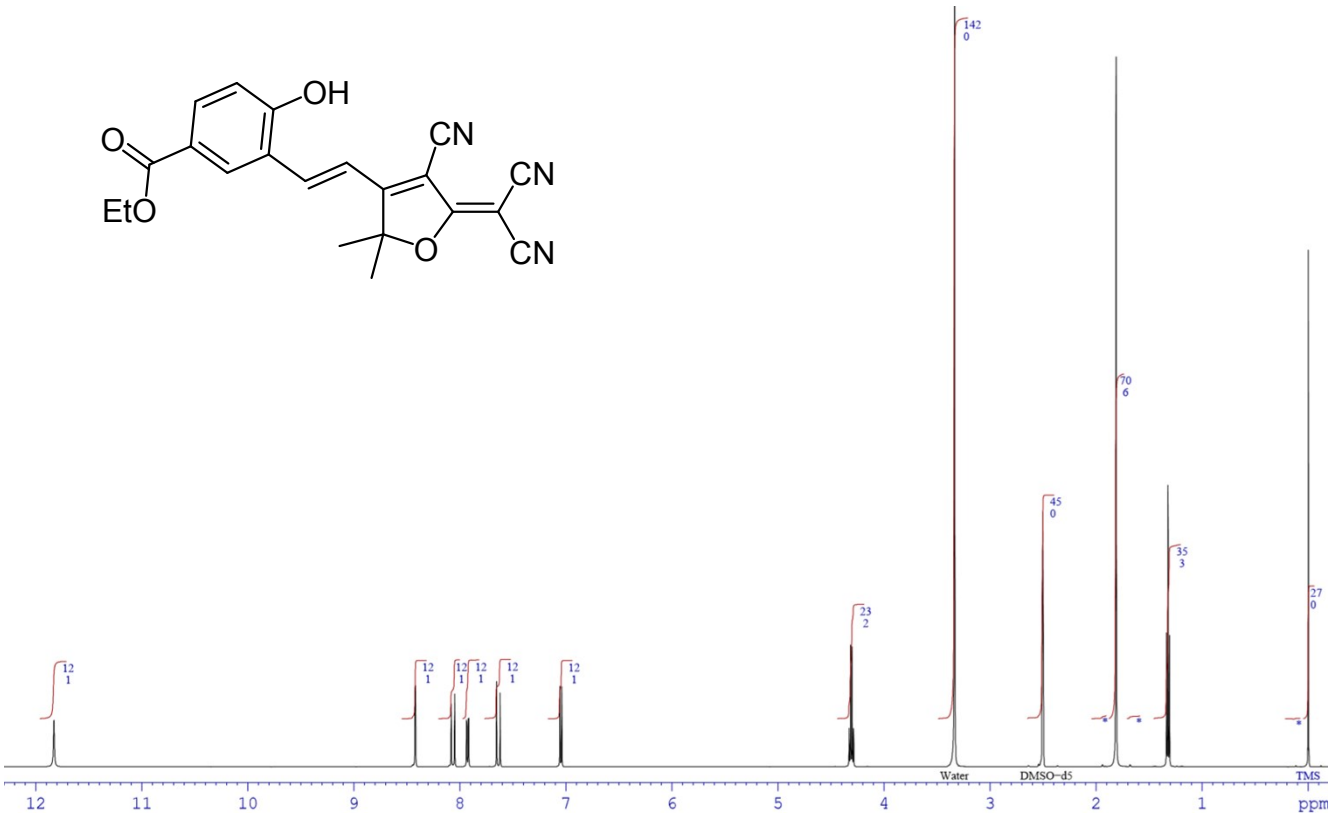

Fig. 15. ^{1}H-NMR-spectrum of compound **1b** (500 MHz, DMSO−d_6, 298K)

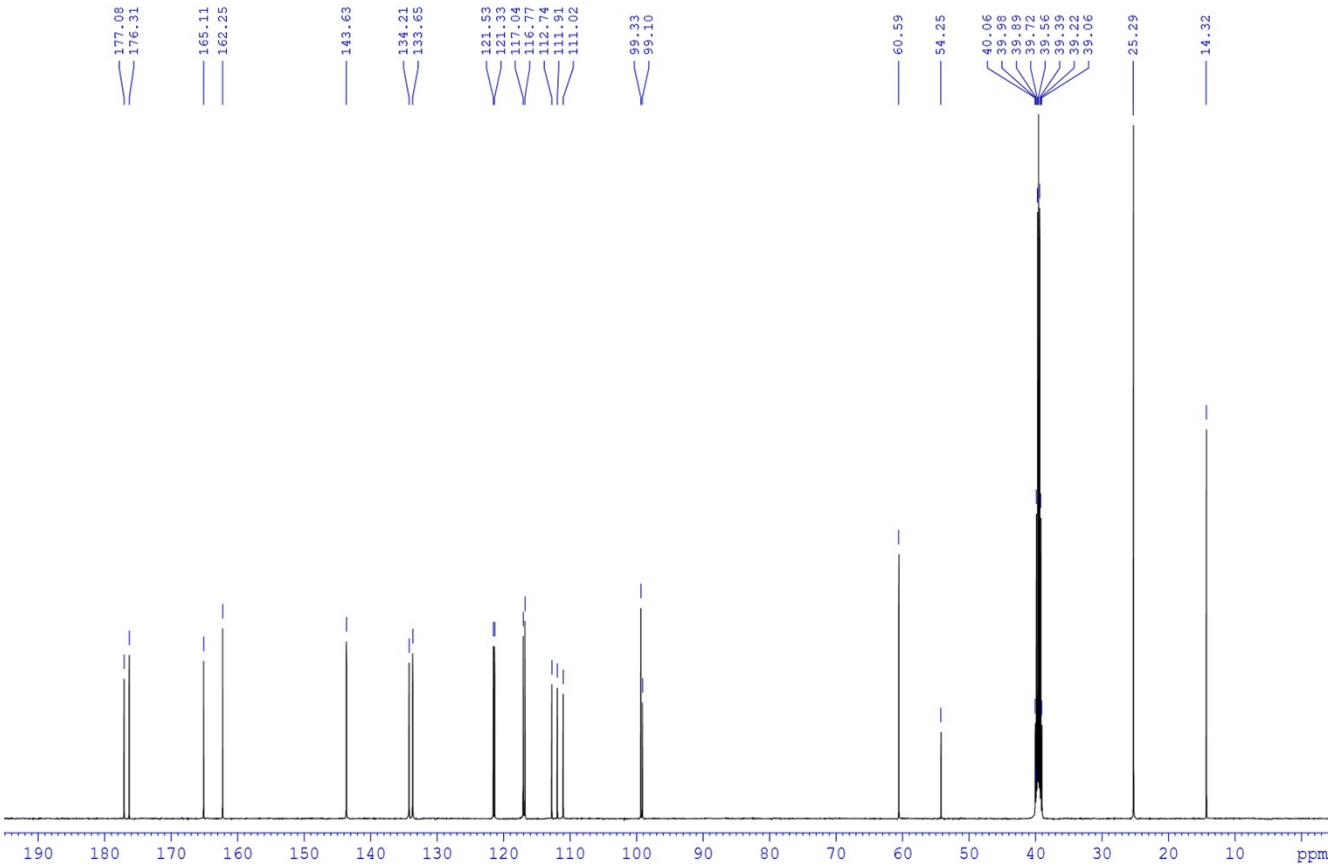

Fig. 16. ^{13}C-NMR-spectrum of compound **1b** (126 MHz, DMSO−d_6, 298K)

4. DFT calculations

Geometry optimization of the compounds was performed using Becke-3-Lee-Yang-Parr (B3LYP) functional with 6-311++G(d,p) basis set in gas phase. The frontier molecular orbitals were visualized using Avogadro software.

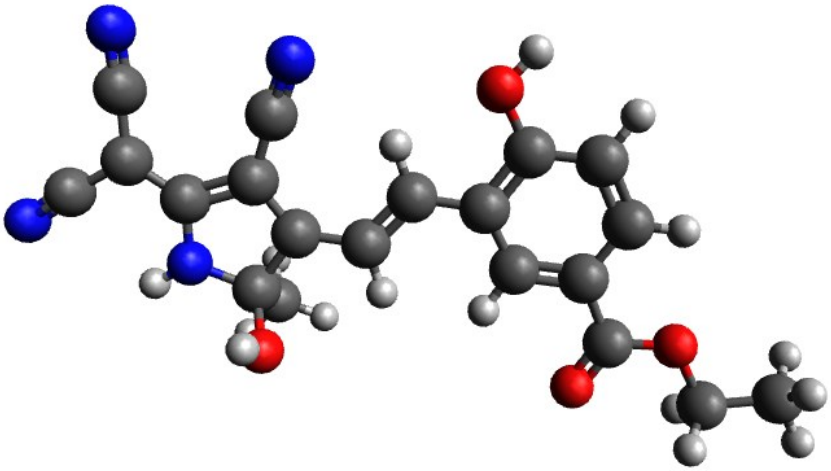

Fig. 17. Optimized geometry of compound **1a**

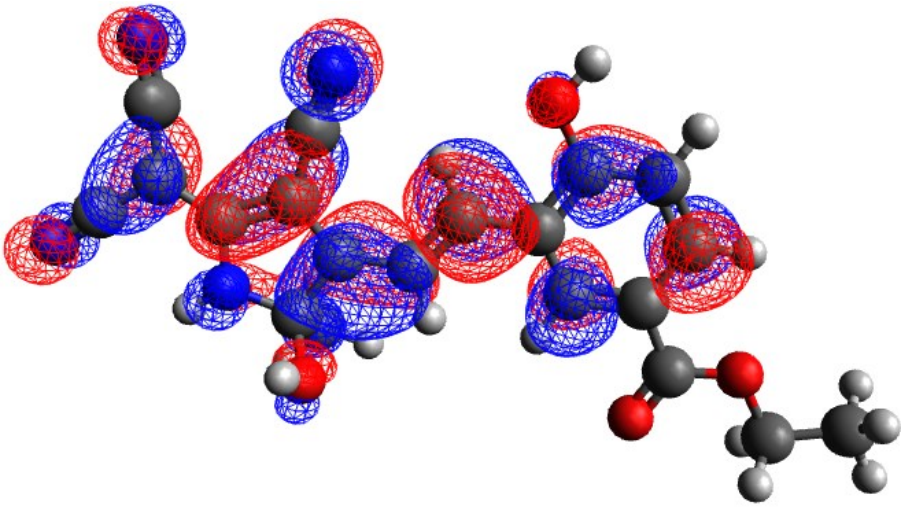

Fig. 18. Visualization of LUMO of compound **1a**

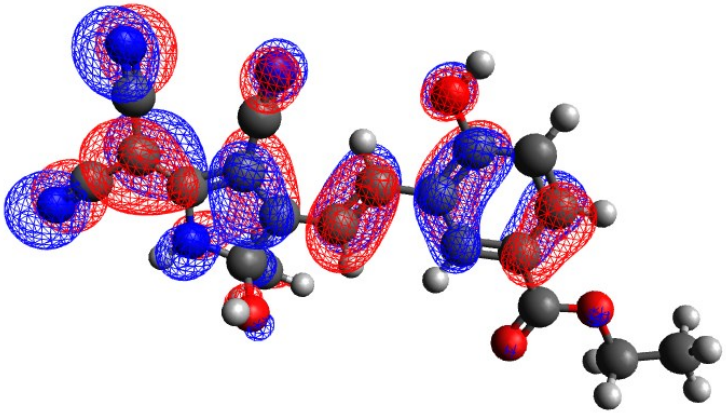

Fig. 19. Visualization of HOMO of compound **1a**

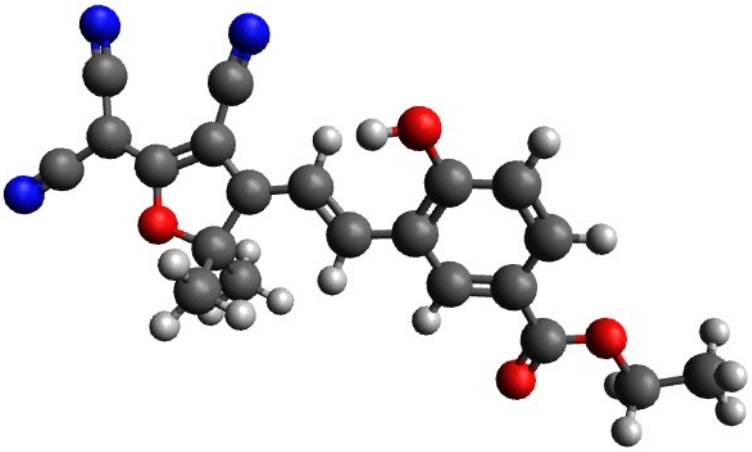

Fig. 20. Optimized geometry of compound **1b**

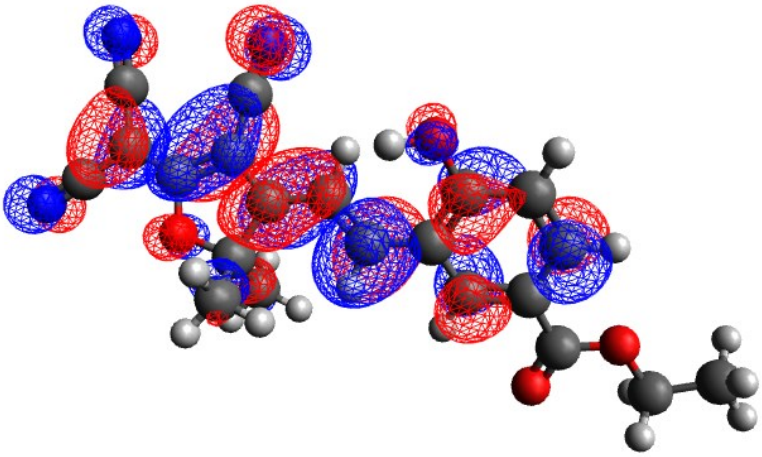

Fig. 21. Visualization of LUMO of compound **1b**

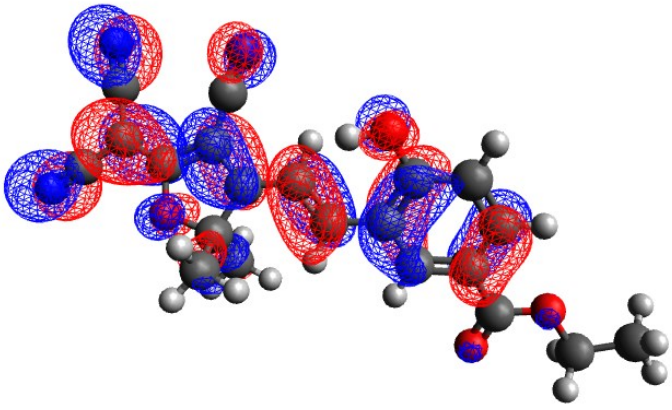

Fig. 22. Visualization of HOMO of compound **1b**